Quest Journals
Journal of Research in Environmental and Earth Sciences
Volume 7 ~ Issue 7 (2021) pp: 08-26
ISSN(Online) :2348-2532
www.questjournals.org

Research Paper

Paleomagnetism of Early Cretaceous Rocks from Nigrub Ring Complexes, South Eastern Desert, Egypt.

Mostafa, R.*; Abd El- All, E.*; Abdeldayem, A. **; El-Hemaly, I.*; Oda, H.*; Awad, A.*

**National Research Institute of Astronomy and Geophysics, Helwan, Cairo, Egypt.*
***Geology Department, Faculty of Science, Tanta University, Tanta.*

Abstract
This study summarizes the rock magnetic, paleomagnetic and magnetic fabric characteristics of Gebel Nigrub El Fogany (139±15 Ma) and Gebel Nigrub El Tahtany (140±15 Ma) ring complexes that occur within the basement of the south Eastern Desert of Egypt. The results of this study establish a new paleomagnetic pole of this era. Rock magnetic measurements performed on these rocks reveal the coexistence of goethite with magnetite and titanomagnetite, which represents the main magnetic carrier. Magnetic fabric studies show that most parts of the complexes are still holding their primary fabric. These rocks are depicting by a weak foliated fabric that shows no signs of high degree of deformation. Demagnetization processes of Nigrub El Fogany and Nigrub El Tahtany ring complexes reveal a single magnetic component of primary origin that reflects the age of these complexes. The characteristic remanent magnetization (ChRM) component isolated from Nigrub El Fogany ring complex has an overall mean direction of D/I = 323°/25°, with k = 17 and α_{95} = 11.9°. This direction corresponds to the north paleomagnetic pole at the Lat. 54°N and Long. 296°E, with K= 17.4 and A_{95} = 12.7. The characteristic remanent magnetization (ChRM) component isolated from Nigrub El Tahtany ring complex has an overall mean direction of D/I = 318°/25°, with k = 46 and α_{95} = 8.8. This direction corresponds to the north paleomagnetic pole at the Lat. 49°N and Long. 298°E, with K= 45.6 and A_{95} = 9. The consistency of resultant poles with the Cretaceous poles from Egypt and Africa indicates the primary origin of these magnetic components.

Keywords: *South Eastern Desert of Egypt, Nigrub Ring complexes, Cretaceous, paleomagnetism, rock magnetism, Magnetic fabrics.*

Received 20 June, 2021; Revised: 03 July, 2021; Accepted 05 July, 2021 © The author(s) 2021. Published with open access at www.questjournals.org

I. INTRODUCTION

Ring complexes in Egypt stayed the subject of several geological, petrological, and geochronological studies especially in the last two decades. The ring complexes of the south Eastern Desert of Egypt are comparable in composition and relationship to those found in Africa ***(Vail, 1968; Marsh, 1973; Neary et al. 1976; Klerkx and Rundle, 1976; Fleck et al., 1976; Foland and Faul, 1977).*** The evaluation of Egyptian ring complexes is still a matter of controversy. ***El Ramly and Hussein (1984)*** assigned the ring complexes of Egypt range in age from Cambrian (554 Ma) to Late Cretaceous (89 Ma), with a wide variety of rock types, ranging from basic to acidic.

This work is a continuation of the paleomagnetic work carried by ***Abdel All, E. (2004)*** and ***Mostafa, R. (2010)***. This study summarizes the results of rock-magnetic, magnetic fabric and paleomagnetic investigations of two well-dated alkaline rock masses (ring complexes); namely Gebel Nigrub El Fogany (NF) (139±15 Ma) and Gebel Nigrub El Tahtany (NT) (140±15 Ma), located in the south Eastern Desert of Egypt, to give clear information about the directions of the geomagnetic field in the Cretaceous age of the rocks under study as well as the positions of the magnetic poles (Paleomagnetic poles) during these geological times, isolate and interpret the different magnetic components constituting the Natural Remanent Magnetization (NRM) of the samples and to identify their carriers.

In this study, we are dealing with two alkaline ring complexes; Gebel Nigrub El Tahtani (NT), and Gebel Nigrub El Fogani (NF) which occur within the basement of the south Eastern Desert of Egypt. They are

located in the central part of the South-Eastern Desert, mid-way between the Nile Valley and the Red Sea coast. **Figure (1)** shows seventeen ring structures identified in the Egyptian Eastern Desert (***El Ramly et al., 1979***).

The topographic relief of the area including the two ring complexes is not simple. Overall, most of the wadis are broad, smooth and covered by compressed debris with patches of hardly passable sands. These wadis separate the rock massive into series of separate relics.

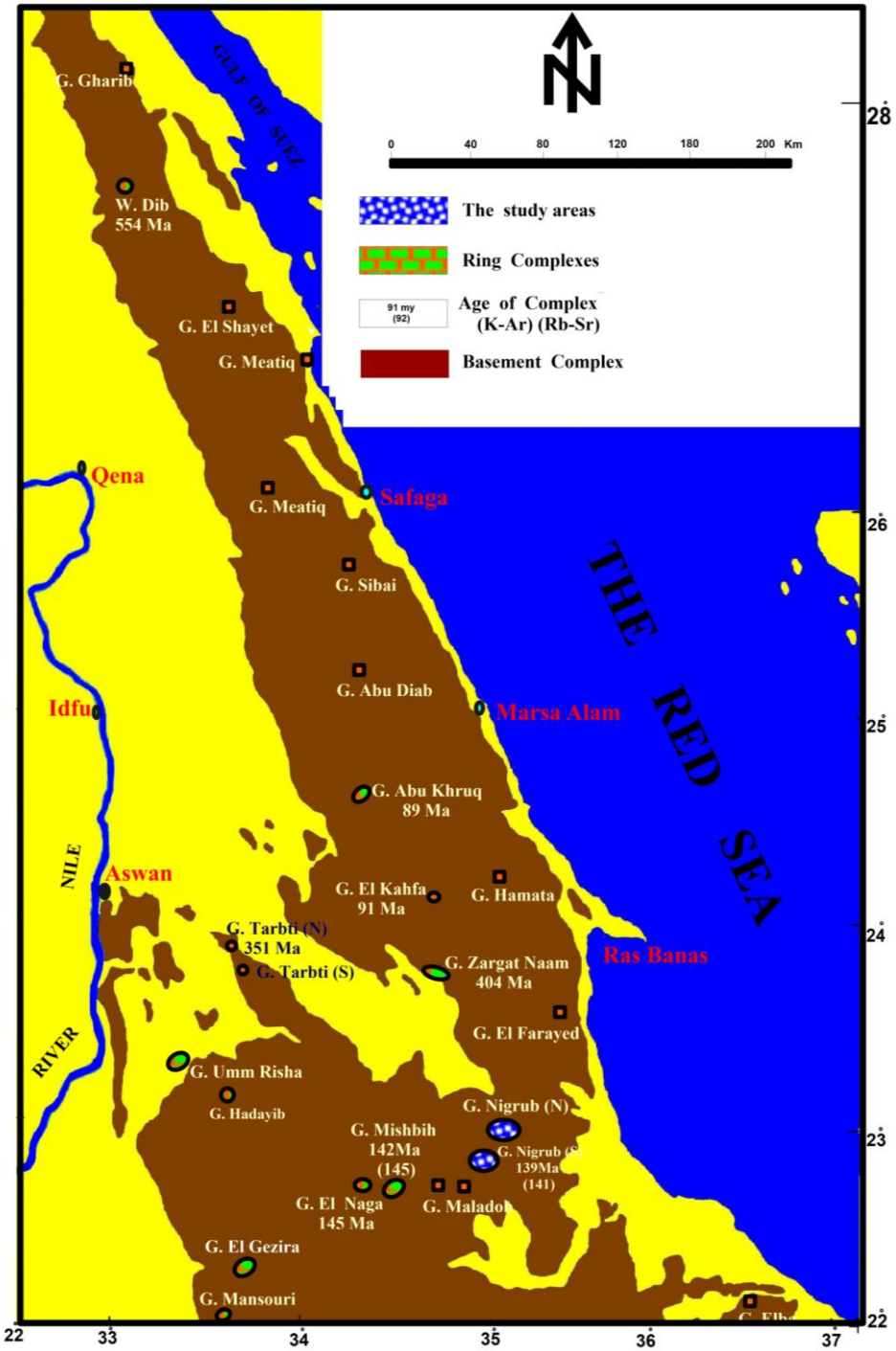

Fig. 1: The distribution of ring complexes in the Eastern Desert of Egypt (modified after El Ramly et al., 1979) and location of the studied rings.

a. Geological setting of Gabal Nigrub El Fogany ring complex

Gabal Nigrub El Fogany is situated on the eastern side of wadi El-Gemmal, south Eastern Desert (see Fig. 1). It is of Late Jurassic-Early Cretaceous (139±15 Ma) age ***(El Ramly et al., 1963)***. Its peak rises up to 1078 m above sea level and lies at the intersection of the latitude 22° 51' 29" N and the longitude 34° 56' 49" E ***(El Ramly et al., 1969)***.

This complex is built up of the relics of a volcanic cone, an inner ring, an outer incomplete ring, and a central stock **(Fig. 2)**. The ring nature of the central stock is indicated by its enclosure of an arch shaped central wadi that drains westward into the ring wadi: – The central stock is composed of various nepheline syenites with their altered varieties. – The central stock-like form of the massif is complicated by the presence of a trochoidal character assuming conical shape. – The volcanic cone is formed of trachytic and rhyolitic lavas and agglomerates, cut by bodies of alkaline gabbro and nepheline syenites. – The part of the outer ring, which is still preserved, is composed of alkaline granites ***(El Ramly et al., 1969)***.

b. Geological setting of Gabal Nigrub El Tahtany ring complex

Gabal Nigrub El Tahtany occurs to the north of Gabal Nigrub El Fogany, and belongs to the Late Jurassic-Early Cretaceous (140±15 Ma) age ***(El Ramly et al., 1979)***. It is a short ridge slightly concave to the southeast **(Fig. 3)** that lies at the intersection of latitude 23° 0' 32" N, and longitude 35° 0' 53" E. At about 10 km to the north of the ridge, sandstones and conglomerates of the Nubian Formation overlie unconformable the metavolcanics.

The main alkaline syenite mass was cut by a series of north western faults, along which the complex is displaced. The amplitude of this displacement reaches 200 m; along these faults, the volcanic rocks are preserved: – The concave ridge is composed of pinkish and greenish gray alkaline syenites. – Volcanic rocks are represented by agglomerates of trachyte and rhyolite. – The country rocks are represented by metavolcanics and schists cut by gray and pink granites ***(El Ramly et al., 1969)***.

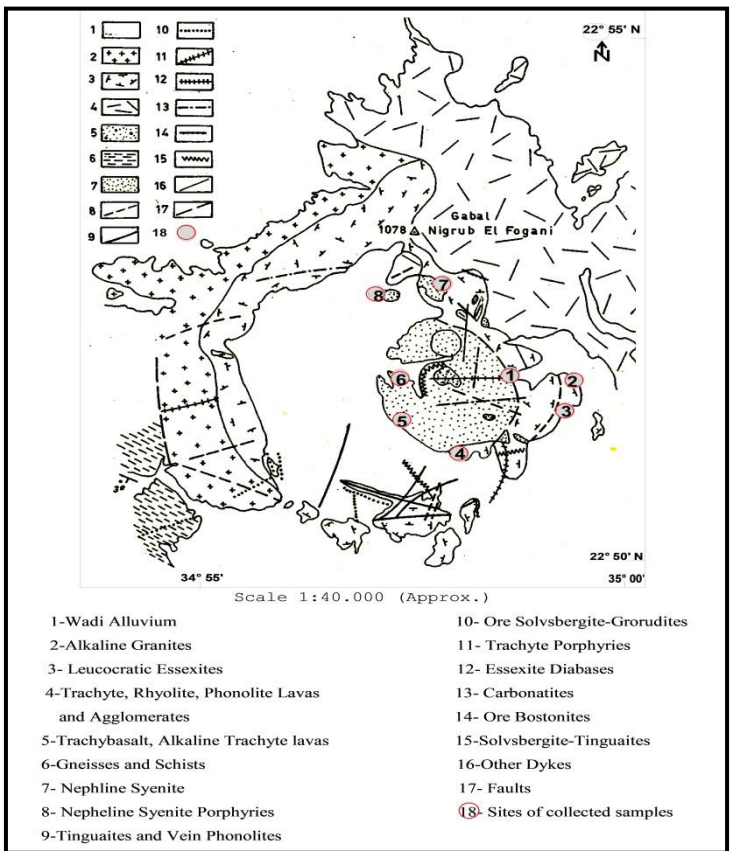

Fig. 2: Photogeological map of Gabal Nigrub El Fogany (after El Ramly et al., 1969) and location of the collected samples.

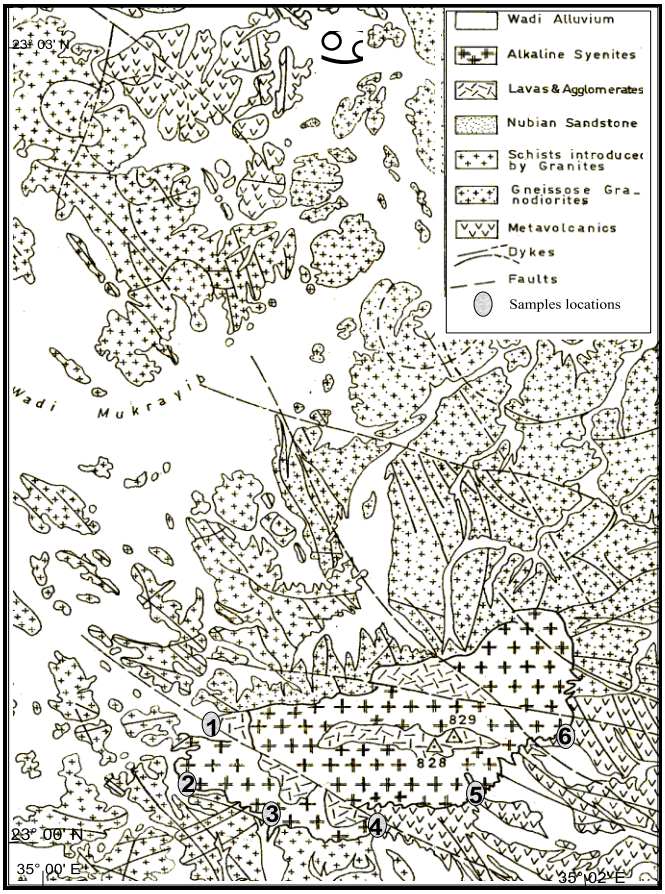

Fig. 3: Photogeological map of Gabal Nigrub El Tahtany (after El Ramly et al., 1979) and locations of the collected samples.

To achieve the goal of this study, the following standard paleomagnetic and rock magnetic investigations were performed:

1) Field sampling of oriented rock blocks from the two rings and laboratory preparation of the drilled cores from these samples.
2) Rock magnetic investigations including Isothermal remanent magnetization (IRM), hysteresis and Curie temperature measurements to identify the predominant magnetic minerals responsible for carrying the magnetization.
3) AMS measurements, including magnetic susceptibility and anisotropy to give information about the petrofabric characteristics and tectonic features of the rocks.
4) NRM measurements and demagnetization (alternating field and thermal) to isolate the different magnetic components.
5) Calculation of the geomagnetic pole positions and their correlation with the corresponding reference poles of Egypt and Africa.
6) Interpreting the obtained results considering available geological information for the two ring complexes.
7) Discussing the possibility of adding the obtained results to the global paleomagnetic database.

II. SAMPLING AND LABORATORY PROCEDURES

Twenty-one oriented hand samples were collected from eight sites at four locations from Nigrub El Fogany Ring Complex **(**see **Fig. 2)**, and twenty-three oriented hand samples were collected from six sites at four locations from Nigrub El Tahtany Ring Complex **(**see **Fig. 3)**.

In the laboratory, one-inch core samples have been drilled and then cut into standard specimens with dimension (2.5 X 2.2cm) **(Fig. 4).** The measurements have been performed in the National Research Institute of Astronomy and Geophysics (NRIAG), Helwan, Egypt and Department of Earth and Planetary Science, University of Tokyo, Japan

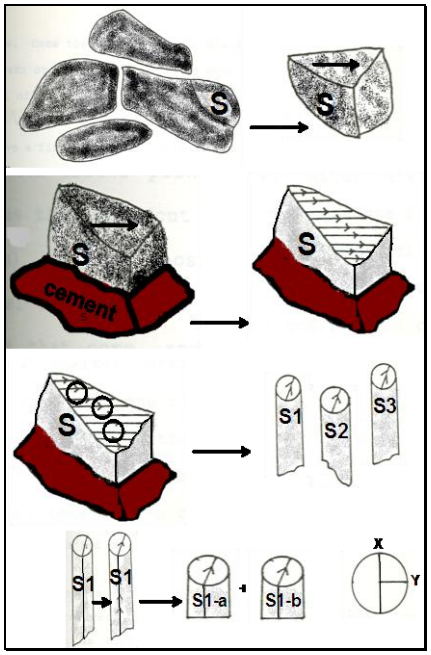

Fig. 4: Steps of specimen orientation and preparation.

Several rock magnetic experiments have been performed to identify the magnetic minerals that could be responsible for magnetization; including measuring the Natural Remanent Magnetization (NRM), construction of Isothermal remanent magnetization (IRM) acquisition curve, Back field determination, Hysteresis Loops and Curie temperature determination (Thermomagnetic analysis). All samples were subjected to stepwise thermal (TH) and alternating field (AF) demagnetization. Vector components were identified from visual inspection of demagnetization diagrams (***Zijderveld, 1967***), and directions have been calculated using principal component analysis (PCA) (***Kirschvink, 1980***). Site means were calculated using Fisher statistics (***Fisher, 1953***).

III. ROCK MAGNETIC RESULTS

The preliminary natural remanent magnetization (NRM) intensities for all specimens have been measured using the JR-6 spinner magnetometer. It ranges from $0.1x10^{-5}$ to $0.3x10^{-3}$ (A/m) in Nigrub El Fogany ring complex and ranges from $0.1x10^{-5}$ to $0.3x10^{-3}$ (A/m) in Nigrub El Tahtany ring complex.
Several rock magnetic experiments were performed to identify the magnetic mineral (s) responsible for carrying magnetization.

a. Thermomagnetic analysis (Js-T curve)

In Nigrub El Fogany Ring Complex, the specimens showed two behaviors **(Fig. 5)**. Most specimens (e.g. NF29 and NF34) showed temperature drops at 50-100°C and was destroyed at temperatures above 600°C, indicating goethite and hematite, while the remaining specimens (e.g. NF25) displayed a temperature destroyed at temperature below 600°C, indicating magnetite.

In Nigrub El Tahtany Ring Complex, the specimens also showed two behaviors **(Fig. 5).** In the first one (e.g. NT17), the curve shows temperature drops at 100°C, 350°C, and 580°C, this indicates magnetite, titanium rich titanomagnetite and goethite. In the second behavior (e.g. NT5 and NT15), there were clear temperature drops at 100°C and > 600°C, There was also a loss of 50% of magnetization during the cooling phase that was probably due to the oxidation of titanomagnetite to hematite.

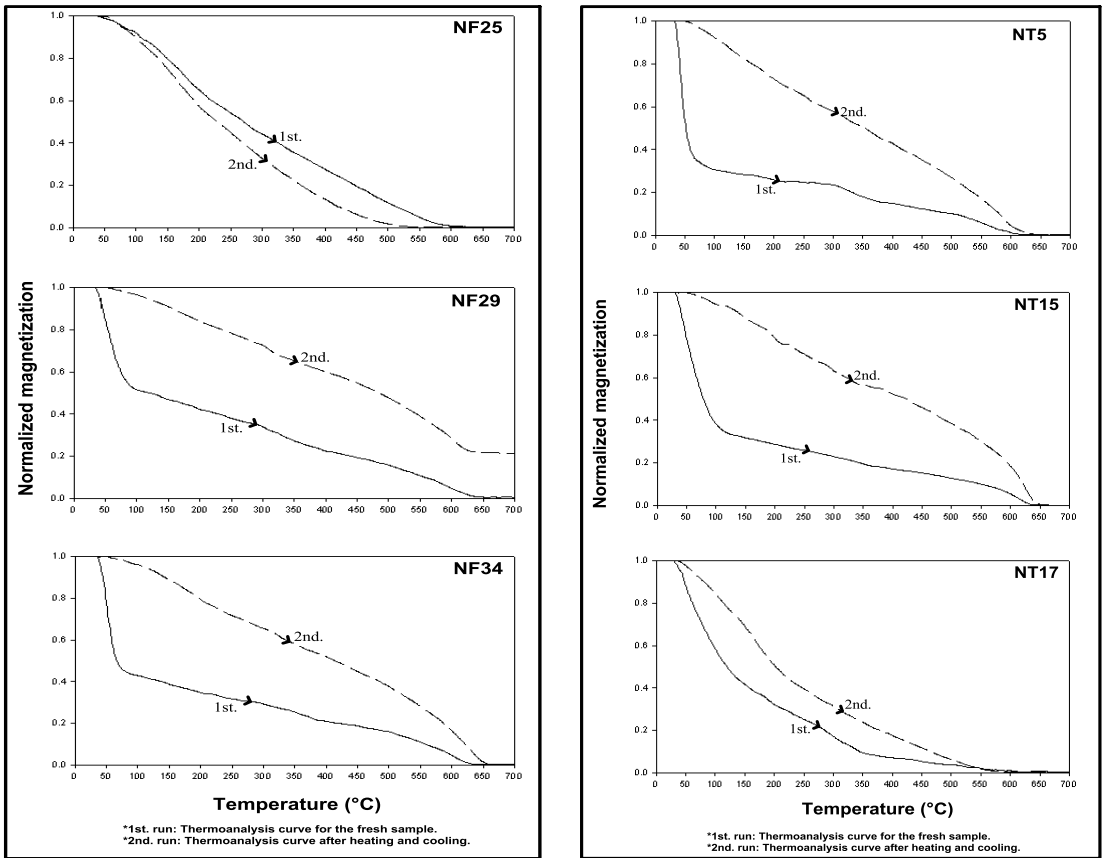

Fig. 5: Thermomagnetic curves for representative specimens from Nigrub El Fogany (NF) and Nigrub El Tahtany ring complexes (NT).

b. Isothermal remanent magnetization (IRM) acquisition analysis

Samples from Nigrub El Fogany and Nigrub El Tahtany ring complexes were subjected to progressive IRM analysis using the Pulls Magnetizer (MMPM10); **Figure (6)** shows the IRM acquisition curves of representative samples from Nigrub El Fogany and Nigrub El Tahtany ring complex.

The constructed curves of specimens from Nigrub El Fogany Ring Complex (e.g. NF25 and NF29) did not reach the saturation state that indicating high coercive mineral (hematite). However, specimens from Nigrub El Tahtany ring complex, showed two behaviors. The first one (e.g. NT17) acquired > 90% of magnetization at 150 mT and reached the saturation state at 300 mT indicating soft magnetic minerals (mainly magnetite). The second one (e.g. NT15) does not reach saturation up to 500 mT, which indicates of presence of high coercive mineral.

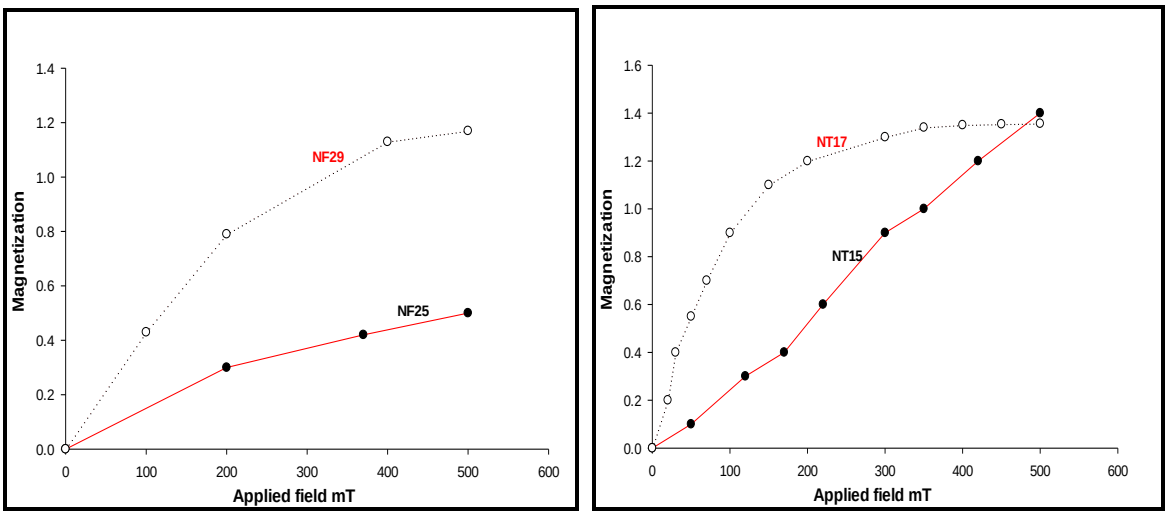

Fig. 6: IRM acquisition curves of representative specimens from Nigrub El Fogany and Nigrub El Tahtany ring complexes.

c. back-field curves

By using the Pulls Magnetizer (MMPM10); the coercivity of remanence (*Hcr*), determined from the back-field curves for most specimens from Nigrub El Fogany ring complex **(Fig. 7)** was found over 100 mT (e.g. NF29). It indicated high coercivity magnetic mineral. Few specimens (e.g. NF25) had values < 100 mT, revealing the existence of low coercive minerals (e.g. titanomagnetite).

The coercivity of remanence (*Hcr*) for some specimens from Nigrub El Tahtany Ring Complex **(Fig. 7)** was found over 200 mT (e.g. NT15). It indicated highly coercive magnetic minerals. In some other specimens (e.g. NT10 and NT17) it was around 50 mT, indicating low coercive magnetic mineral.

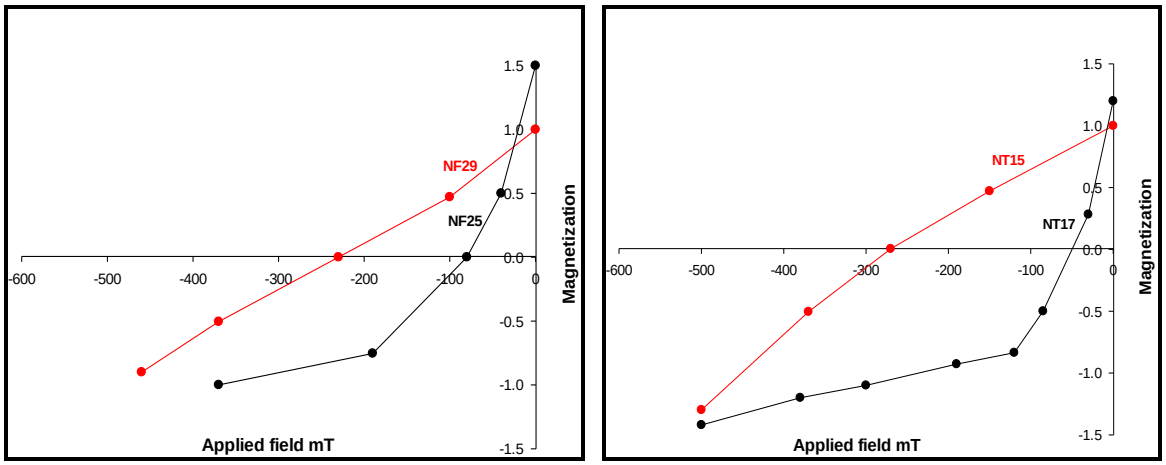

Fig. 7: Back-field curves of representative specimens from Nigrub El Fogany and Nigrub El Tahtany ring complexes.

d. Hysteresis loop analysis

The hysteresis properties of representative specimens from different sites of Nigrub El Fogany Ring Complex are shown in **Figure (8)**. These loops are of wasp tail shape. A typical example of hysteresis curve is shown for specimens (NF25), where a complete saturation was achieved at 400 mT, with narrow curves that indicate titanomagnetite and magnetite. In other sites, incomplete saturation was encountered (e.g. NF29). The wasp tail shapes reveal more than one magnetic mineral and the wide incomplete saturation curve reflects hematite presence.

The hysteresis properties of representative samples from different sites of Nigrub El Tahtany Ring Complex are shown in **Figure (8).** Similar to those from Nigrub El Fogany Ring Complex, these specimens showed wasp tail shape loops revealing two magnetic minerals, with low coercivity force (*Hc*) and low values of saturation remanence. A typical example is shown for specimens (NT17). It displays complete saturation at 500 mT, with simple narrow curve. In other sites, incomplete saturation up to 700 mT was not achieved (e.g. NT10) with wasp tail and wide curve (reflects hematite presence).

The magnetic granulometry technique using hysteresis loop properties was used to estimate the magnetic mineral grain size in the study rocks. **Figure (9)** shows the ratio of saturation remanence to saturation magnetization of Nigrub El Fogany and Nigrub El Tahtany ring complexes (*Mrs/Ms*) to range from 0.1 to 0.3, and that of coercivity of remanence to coercive force (*Hcr/Hc*) to range from 2.0 to 4.0 on the Day plot (***Day et al. 1977***). These results indicate that the magnetic grain size of both Nigrub El Fogany and Nigrub El Tahtany ring complexes are within the size range of the pseudo-single domain (PSD). Where, Mr: saturation remanence, Ms: saturation magnetization, Hcr: remanent coercivity, Hc: coercive force, SD: single domain, PSD: Pseudo-single domain and MD: Multidomain.

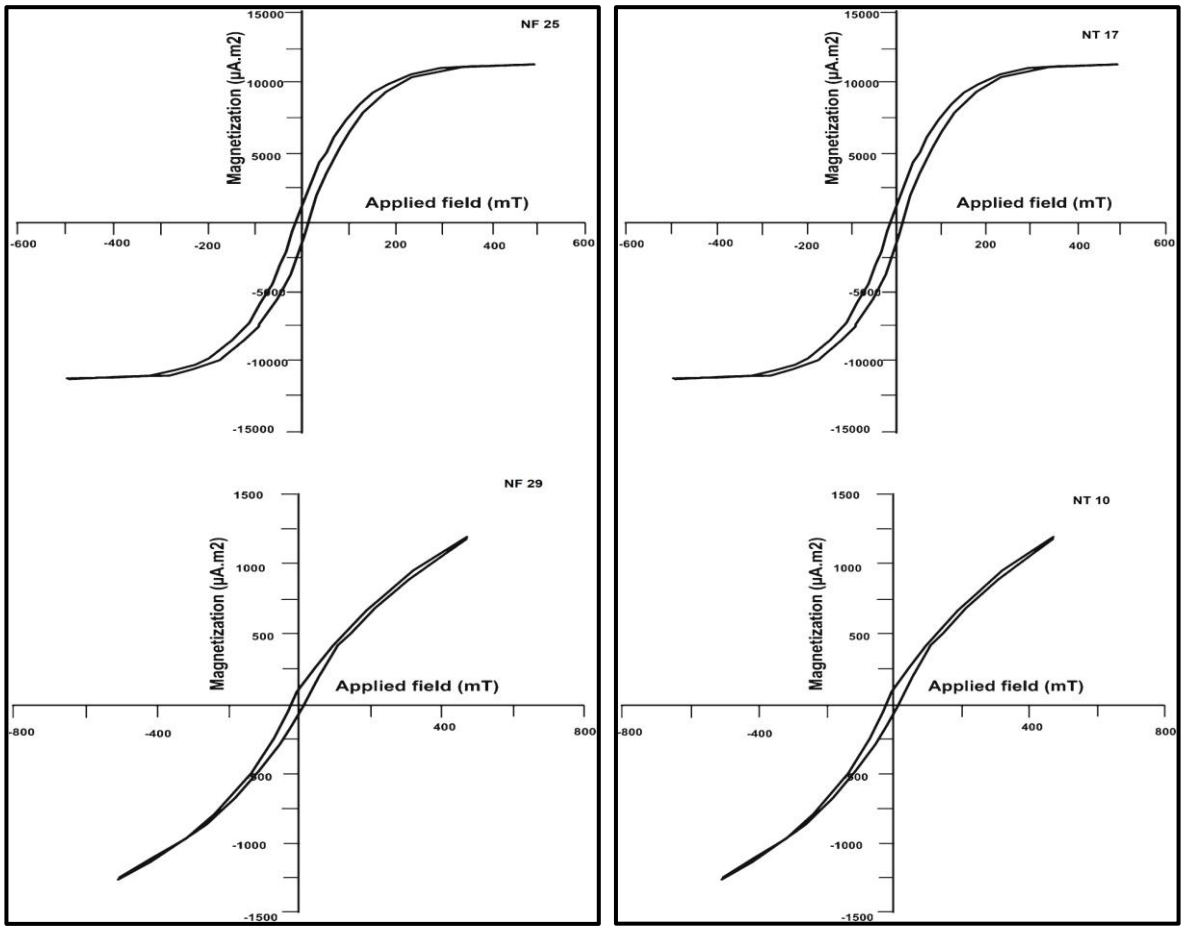

Fig. 8: Hysteresis curves of representative specimens from Nigrub El Fogany and Nigrub El Tahtany ring complexes.

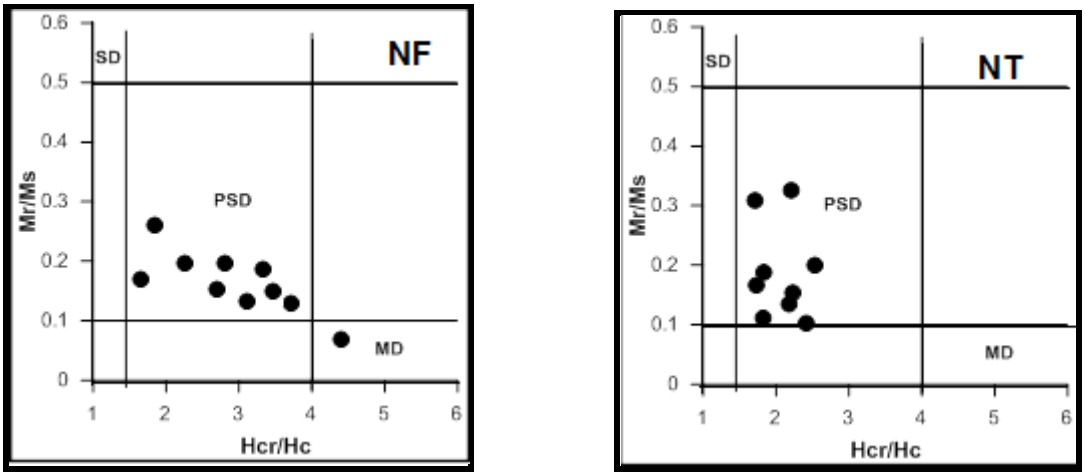

Fig. 9: Day plots for hysteresis data for representative specimens from Nigrub El Fogany and Nigrub El Tahtany ring complexes.

IV. MAGNETIC FABRICS RESULTS

a.Nigrub El Fogany

Measurements of magnetic susceptibility and AMS were performed on 95 standard cylindrical rock specimens, collected from 8 sites distributed throughout the Nigrub El Fogany ring complex.

Table (1) lists the site-mean magnetic susceptibility, AMS parameters magnitudes and axis orientations. As shown in this table, the mean magnetic susceptibility is variable among different sites. The highest values are

recorded in samples from site 7 with a site-mean of 744 x 10^{-6} S.I. units. Samples from sites 2 and 8 gave us the lowest susceptibility values, varying from 50 x 10^{-6} to 73 x 10^{-6} S.I. units, while those from sites 1, 3, 4, 5, and 6 yielded intermediate susceptibility values that vary from 120 x 10^{-6} to 200 x 10^{-6} S.I. units. The overall mean susceptibility of Nigrub El Fogani is 204 x 10^{-6} S.I. units.

The anisotropy degree, P' showed low variable values (**Table 1**) that range from 1.012 to 1.074 with an average sites-mean of 1.040. Samples from sites 2 and 5 gave us the highest P' values (1.070 to 1.074, with an average of 1.072), while those from sites 3, 4, and 8 gave the lowest P' values (1.012 to 1.023, with an average of 1.016).

Table 1: Site-mean magnetic susceptibility and AMS data for Nigrub El Fogany ring complex.

Site	N	K_m (*10^{-6} SI unit)	P'	T	L	F	Magnetic susceptibility axes		
							K_{max}	K_{int}	K_{min}
Site 1	15	200	1.040	0.380	1.011	1.030	114/28	242/47	1/33
Site 2	12	50	1.070	-0.200	1.042	1.030	20/45	359/63	198/25
Site 3	18	125	1.012	0.033	1.010	1.010	125/22	281/34	25/72
Site 4	15	126	1.013	0.440	1.00	1.010	174/37	105/59	281/47
Site 5	9	196	1.074	0.710	1.010	1.060	240/44	269/21	63/70
Site 6	8	120	1.050	-0.064	1.035	1.030	242/26	117/47	1/41
Site 7	12	744	1.040	-0.067	1.022	1.020	16/57	40/12	244/48
Site 8	6	73	1.023	0.048	1.010	1.020	169/5	199/36	40/62
Mean	95	204.25	1.040	0.160	1.025	1.030	-----	-----	-----

Where, ***N***: number of specimens, ***Km***: mean susceptibility = $(K_1 + K_2 + K_3) / 3$, in 10^{-6} SI.

P' or Pj: anisotropy degree = $exp\sqrt{\{2[(\eta_1-\eta_m)^2 + (\eta_2-\eta_m)^2 + (\eta_3-\eta_m)^2}$

Where**:** $\eta_1 = ln\ K_1$, $\eta_2 = ln\ K_2$, $\eta_3 = ln\ K_3$ and $\eta_m = \sqrt[3]{\eta_1.\eta_2.\eta_3}$

T: ellipsoid shape = $[2\ ln\ (K_2 / K_3) / ln\ (K_1 / K_3)] - 1$

L: magnetic lineation = K_1 / K_2, ***F***: magnetic foliation = K_2 / K_3.

The direction of the principal magnetic susceptibility axes is scattered with variable degree of inclination, reflecting a weak magnetic fabric. The K_1 axes (magnetic lineation) are shallow to moderately steep and trend in a scattered broad SE-NW direction. K_2 axes are widely scattered**,** while the K_3 axes (magnetic foliation poles) are scattered along the NE-SW direction, with moderate to steep inclinations **(Fig. 10-a)**. Plots of the anisotropy degree *Pj* against the mean magnetic susceptibility K_m **(Fig. 10-b)** reveal no definitive relationship. The overall site-mean *T* value is 0.160, *i. e.,* in the range of $0 < T \leq 1$, confirming a predominance of foliation over lineation. This is also demonstrated in the *P*j-*T* plot **(Fig. 10-c)** where most samples fall well within the positive *T* field.

The variable magnetic susceptibility of Nigrub El Fogany ring complex reflects variation in content and type of ferromagnetic minerals. The low anisotropy degree *P'* (average of 4.0%) and the predominance of magnetic foliation over lineation with the obtained axial distribution pattern, all indicate that the magnetic fabric of Nigrub El Fogany most probably reflects the original emplacement setting through a magma/lava flowing broadly along the SE-NW direction and subsequent cooling and crystallization in a weak deformational condition.

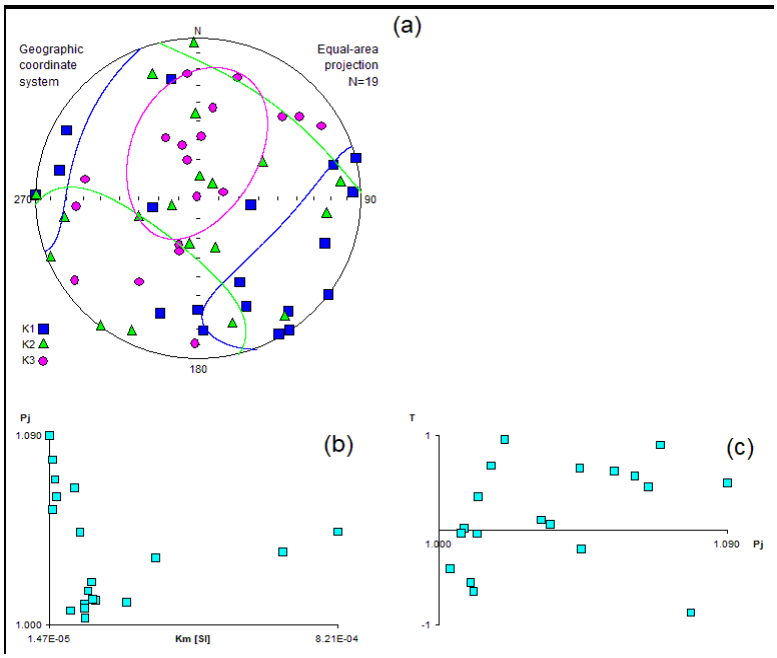

Figure 10: **a**) Equal-area projection of the in-situ directions of magnetic susceptibility principal axes for sites from Nigrub El Fogany ring complex. **b**) Relationship between magnetic susceptibility Km and anisotropy degree Pj and **c**) Relationship between ellipsoid shape T and anisotropy degree P' of samples from Nigrub El Fogany ring complex.

b.Nigrub El Tahtany

Measurements of magnetic susceptibility and AMS were performed for 85 standard cylindrical rock specimens, collected from 6 sites distributed throughout the Nigrub El Tahtany ring complex. **Table (2)** lists the site-mean magnetic susceptibility, AMS parameters magnitudes and axis orientations.

As shown in **Table (2)**, variable magnetic susceptibility magnitudes are obtained from different sites. The highest values are recorded at site 1 (average site-mean is 221 x 10^{-6} S.I. units), while the lowest susceptibility values are recorded at sites 5 and 6 (average is 58.5 x 10^{-6} S.I. units). Sites 2, 3, and 4 yielded intermediate susceptibility values (average is 111 x 10^{-6} S.I. units). The overall mean susceptibility of Nigrub El Tahtany is 112 x 10^{-6} S.I. units.

The anisotropy degree P' showed low variable values that range from 1.011 to 1.04 with an average sites-mean of 1.02 (**Table 2**). Specimens from sites 1, 2, and 6 gave us the highest values (from 1.02 to 1.04, with an average of 1.027). Those from sites 3, 4, and 5 gave us the lowest values (from 1.011 to 1.013, with an average of 1.012).

Table 2: Site-mean magnetic susceptibility and AMS data for Nigrub El Tahtany ring complex.

Site	N	K_m ($*10^{-6}$ SI unit)	P'	T	L	F	Magnetic susceptibility axes		
							K_{max}	K_{int}	K_{min}
Site 1	15	212	1.020	0.133	1.00	1.010	25/52	283/57	154/79
Site 2	8	143	1.020	0.130	1.010	1.010	182/21	119/74	37/62
Site 3	12	91	1.012	0.280	1.00	1.010	51/22	303/29	162/48
Site 4	20	100	1.011	0.190	1.00	1.010	140/33	35/48	234/57
Site 5	6	57	1.013	0.170	1.00	1.010	220/67	168/47	146/62
Site 6	24	60	1.040	0.40	1.010	1.020	48/56	228/61	157/43
Mean	85	112	1.020	0.220	1.00	1.012	------	-----	-----

Notations as in Table (3)

The direction of the principal magnetic susceptibility axes is scattered with variable degree of inclination, reflecting a weak magnetic fabric. The K1 axes (magnetic lineation) are shallow to moderately steep

and trend along a broad NE-SW direction. The K2 axes show wide scatter, while the K3 axes (magnetic foliation poles) are scattered along the SE-NW direction, with moderate to steep inclinations (**Fig. 11-a**).

The relation between the anisotropy degree P' and the mean magnetic susceptibility Km reveals no clear trend (**Fig. 11-b**). The magnetic lineation L and magnetic foliation F are rather weak (**Table 2**), which reflects the predominance of magnetic foliation over lineation.as demonstrated in the relation between foliation F versus lineation L and between the shape parameter T and the anisotropy degree P' (**Fig. 11-c**), where values from most plots fall in the flattening fields.

The variability of magnetic susceptibility reflects differences in the content and type of ferromagnetic minerals carrying the AMS components. The low anisotropy (average of 2.0%) indicates a low degree of deformation with magnetic foliation-predominating lineation. The obtained magnetic fabric pattern, exemplified by weak parameter magnitudes and axial distribution, indicates that Nigrub El Tahtany still holds its primary fabric with respect to the original emplacement setting through magma/lava flowing in a broad NE-SW direction with subsequent cooling and crystallization in a weak compressional condition.

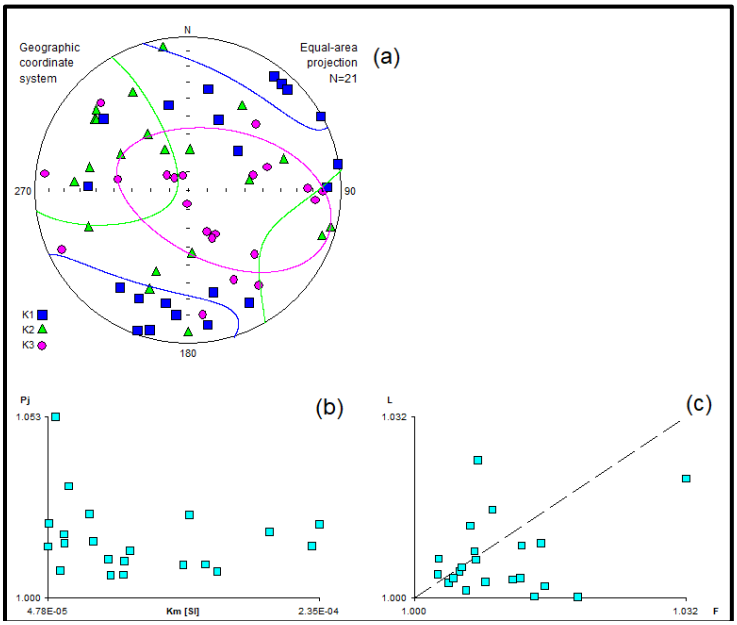

Fig. 11: **a**) Equal-area projection of the in-situ directions of magnetic susceptibility principal axes for sites from Nigrub El Tahtany ring complex**. b**) Relationship between magnetic susceptibility Km and anisotropy degree Pj and **c**) Relationship between ellipsoid shape T and anisotropy degree P' of samples from Nigrub El Tahtany ring complex.

5. Paleomagnetic results

a. Nigrub El Fogany

Specimens from all sites gave low initial values of NRM intensities, with samples from site 4 yielding the lowest initial intensity averaging $0.1x10^{-5}$ A/m, while those from site 6 had the highest initial intensity averaging $0.3x10^{-3}$ A/m.

The stability of magnetization was first tested by subjecting pilot samples from each site to a full-range of demagnetization treatment using both AF and thermal methods. Typical examples of AF demagnetization plots of pilot samples from this complex are shown in **Figure (12)**.

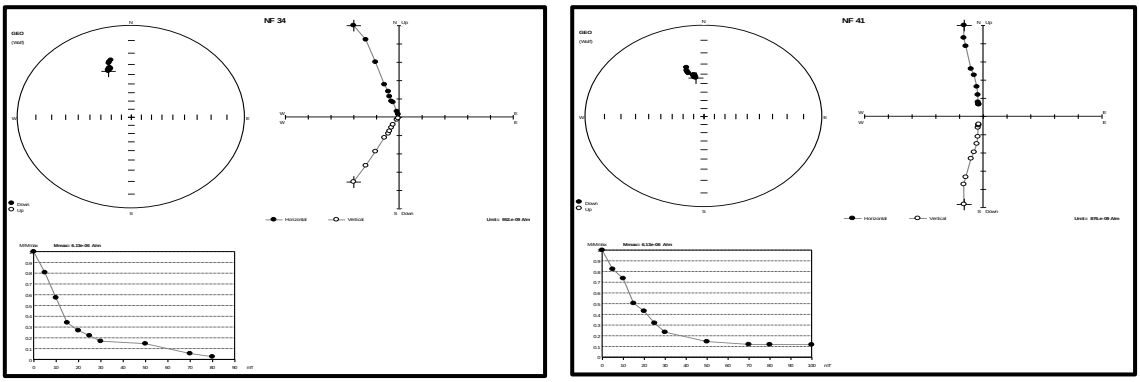

Fig. 12: Typical examples of AF demagnetization plots of samples from Nigrub El Fogany ring complex.

Two manners were observed during AF demagnetization from Nigrub El Fogany ring complex. The first behavior is represented by specimen (NF41), which displayed a univertical decay of NRM direction toward the origin of orthogonal plot. About 85% of the initial NRM of the specimen was removed at the demagnetization field of about 20 mT. This indicates that a low coercive carrier carries the greatest part of NRM. Specimen from sites 1, 2, 7, and 8 belong to this behavior. The NRM of these samples therefore be carried by magnetite rather than hematite. The second behavior, represented by specimen (NF34), is characterized by the isolation of the component at 20 mT with a removal of 90% of the initial NRM. Specimen from sites 3, 4, 5, and 6 belong to this behavior.

As the AF demagnetization was successful in demagnetizing only 70% of the initial NRM intensity of some specimens, thermal demagnetization was also applied on pilot samples from different sites. Typical examples of thermal demagnetization plots of Nigrub El Fogany specimens are shown in **Figure (13)**. During thermal demagnetization, two behaviors were observed. A typical example of the first behavior is represented by specimen (NF41), only a small part of the intensity of remanence (10% of the initial NRM) was removed at the demagnetization temperature of about 100°C, after which, the remaining part of the remanence decreases rapidly until losing about 90% of the initial NRM at 600°C, leading to the isolation of a single component that headed toward the origin. This means that the greatest part of NRM is probably carried by hematite rather than magnetite. The second behavior is more complicated (NF34), as it started with the removal of an unstable component at 100°C, then NRM continued to decay until losing about 80% of its initial value at 600°C with direction heading toward the plot origin. This means that the greatest part of NRM is probably carried by hematite.

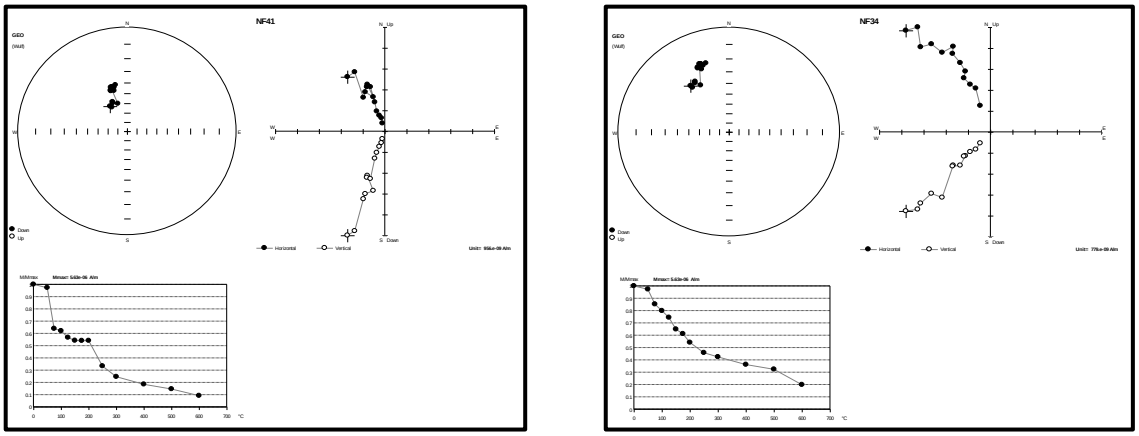

Fig. 13: Typical examples of thermal demagnetization plots of specimens from Nigrub El Fogany ring complex.

b. Nigrub El Tahtany

In this complex, specimens from all sites yielded low initial intensity values ranging from $0.1x10^{-5}$ A/m to $0.3x10^{-3}$ A/m. The representative specimens showed high stability against AF demagnetization. Typical examples of AF demagnetization plots are shown in **Figure (14)**. Only 40% of the initial NRM was removed at the demagnetization field of about 100 mT (e.g. NT20), or 60 mT (e.g. NT16). Above these levels, the slope of the intensity decay curve did not change and the field became ineffective.

Typical examples of thermal demagnetization plots of Nigrub El Tahtany specimens are shown in **Figure (15)**. As the figure shows, two behaviors were observed during heating. In the first one (e.g. specimen NT20 in **figure 15**), a large part of the intensity of remanence was removed at about 400°C, followed by a sharp decay up to 600°C when NRM was destroyed, leading to the isolation of a single component that headed toward the origin of the orthogonal plot **(Fig. 15)**. This means that the largest part of NRM is carried by magnetite.

In the second behavior (represented by specimen NT16 in **figure 15**), large part of the intensity of remanence (70% of the initial NRM) was removed and a soft component was isolated at about 200°C. The remaining part of the remanence then began to decrease slowly to lose about 85% of the initial NRM at 600°C. This means that the greatest part of NRM is carried by goethite while the remaining small part is carried by hematite.

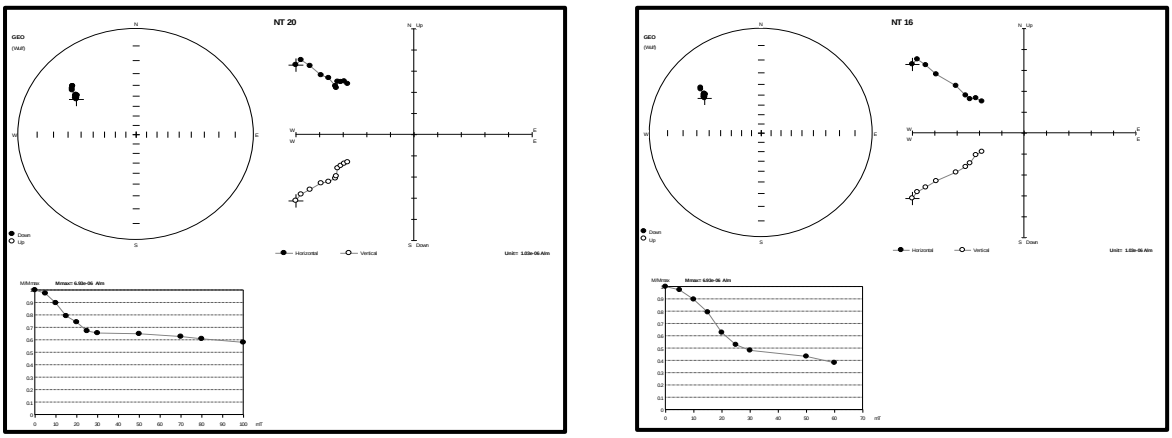

Fig. 14: Typical examples of AF demagnetization plots of specimens from Nigrub El Tahtany ring complex.

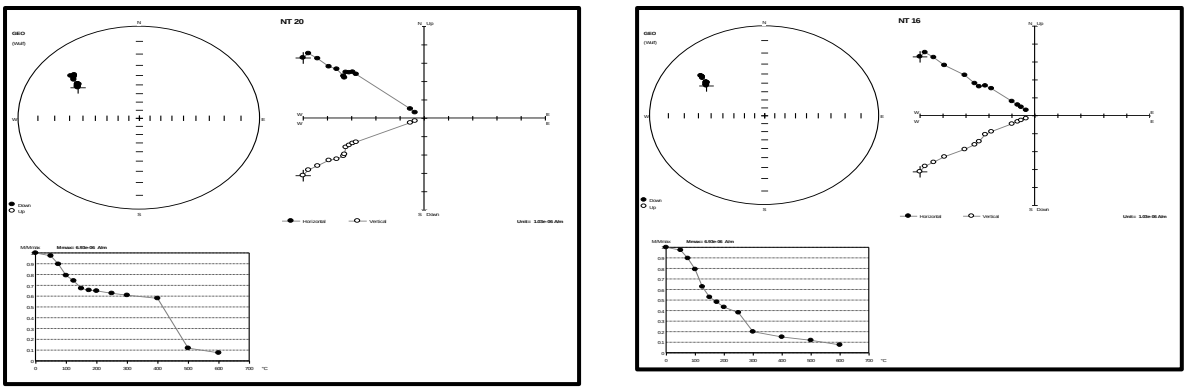

Fig. 15: Typical examples of thermal demagnetization plots of specimens from Nigrub El Tahtany ring complex.

Demagnetization data from specimens were plotted on orthogonal projection (***Zijderveld, 1967***) and line segments were selected to perform principal component analysis (***Kirschvink, 1980***). The resultant site-mean directions and their corresponding virtual geomagnetic poles (VGP) with component-mean directions and equivalent paleomagnetic poles from the different sites were calculated using REMASOFT 3.0 computer program. The obtained results are listed in **Tables (3&4)** and plotted in **Figures (16&17)**.

Table 3: Site and component-mean ChRM and secondary NRM data and corresponding virtual paleomagnetic poles for Nigrub El Fogany ring Complex.
(Location 22° 51' N and 34° 55' E)

Site/Component	N	*ChRM*		*VGP*
		D(°) I(°)	**α_{95} (°) k**	**Long. Lat.**
Component A				
Site 1	3	319 10	11 23	299 54
Site 3	3	312 18 327 40	11.2 20 9.3 16.5	296 42 280 49
Site 4	3	309 12 339 19	5.0 27.3 12 15.6	286 66 279 44
Site 5	3	312 27	6.1 28.9	251 64
Site 6	2	342 40	8 27.4	270 59
Site 7	3	340 37 315 16	11.2 14 10.4 15	263 50 288 52
Mean (6)	17	323 25	11.9 17	***PP*** **Long. Lat.** 296 54 A_{95}=12.7 K=17.4
Component B				
Site 2	2	170 22 180 27	5.3 40 3.8 44	60 -50 49 -59
Site 6	2	172 2	9 60	55 -52
Site 7	3	161 17	7.2 80	51 -56
Site 8	2	170 19 168 15	11.2 77 9.8 51	53 -55 57 -51
Mean (4)	9	170 17	7.3 60.9	***PP*** **Long. Lat.** 233 57 A_{95} =8.5 K=62.8

N: number of samples in each site, **D & I**: Magnetic declination and inclination angles, in degrees; **K**, **α_{95}** & **A_{95}**: precision parameter and semi-angle cone of 95% confidence about site- and component- mean direction (Fisher, 1953); **Lat.** & **Long.**: latitude and longitude of the Virtual (VGP) and paleomagnetic (PP) pole position.

Table 4: Site and component-mean ChRM and secondary NRM data and corresponding virtual paleomagnetic poles for Nigrub El Thtany ring Complex.
(Location 23° 01' N and 35° 00' E)

Site/Component	N	*ChRM*		*VGP*
		D(°) I(°)	**α_{95} (°) k**	**Long. Lat.**
Component A				
Site 1	3	312 23	12 70	290 50
Site 2	2	322 22	13.2 31	277 48
Site 3	3	319 18	4.6 27	286 44
Site 4	5	309 22	5.3 44	299 47
Site 5	2	316 20	3.8 69	293 53
Site 6	8	328 32 311 29	7.1 39 9 66	287 49 293 51
Mean (6)	23	318 25	8.8 46	***PP*** **Long.** 298 **Lat.** 49 A_{95} =9 K=45.6
Component B				
Site 3	3	16 20	5.3 21	159 66
Site 4	5	23 21 12 6	9.0 60.6 6.8 70	162 64 166 65

Site 6	8	18 31 20 11	11 44.8 14 51	164 69 161 66
Mean (3)	16	18 18	9 62	***PP*** **Long. 161 Lat. 68** A_{95} = 9.9 K=60.1

Notations as in Table (4)

In addition to this Earth's field component, two main magnetic components could be isolated from Nigrub El Fogany ring complex; one is considered the ChRM **Component (A)** and the other **Component (B)** is a secondary**. Component (A)** was isolated from all sites except sites 2 and 8, during either AF demagnetization between 80 and 120 mT; or during thermal demagnetization between 300 and 600°C. The site-mean ChRM directions show shallow to moderate inclinations with normal polarities that are predominantly directed to the NNW. The mean ChRM direction is *D/I* = 323°/25°, with *k* = 17 and α_{95} = 11.9° (**Table 3)**. This direction corresponds to a paleomagnetic pole at the *Lat.* 54°°N and *Long.* 296°E, with *K*= 17.4 and A_{95} = 12.7 **(Fig. 16)**.

The second **Component (B)** was recorded in samples from sites 2, 6, 7, and 8, isolated during either AF demagnetization at ranges between 15 and 50 mT, or thermal demagnetization between 120 and 300°C. It has shallow inclinations with normal polarities that are predominantly directed to the S. The mean direction is *D/I* = 170°/17°, with *k* = 61 and α_{95} = 7.3 (**Table 3)**. This direction corresponds to a north paleomagnetic poles at the *Lat.* 57°N and *Long.* 233°E, with *K*= 62.8 and A_{95} = 8.5 **(Fig. 16)**. As **Component (B)** was removed before isolating **Component (A)**, the latter is believed to be older and as it heads toward the plot origin up to the end of treatment. **Figure (17)** displays the plots of the corresponding paleomagnetic poles from the two components.

Two well-defined magnetic components are also identified from Nigrub El Tahtany ring complex **(Table 4)**. One is considered the ChRM **Component (A)** and the other **Component (B)** is a secondary.

Component (A) was isolated from all sites; during either AF demagnetization between 50 and 130 mT; or during thermal demagnetization between 580 and 680°C. The site-mean ChRM directions show shallow to moderate inclinations with normal polarities that are predominantly directed to the NNW. The mean ChRM direction is *D/I* = 318°/25°, with *k* = 46 and α_{95} = 8.8. This direction corresponds to paleomagnetic poles at the *Lat.* 49°N and *Long.* 298°E, with *K*= 45.6 and A_{95} = 9. **(Table 4** and **Figure 18)**.

The second **Component (B)** was recorded in samples from sites 3, 4, and 6, isolated during either AF demagnetization at ranges between 15 and 20 mT, or thermal demagnetization between 100 and 250°C. It has shallow inclinations with normal polarities that are predominantly directed to the N. The mean direction is *D/I* = 18°/18°, with *k* = 62 and α_{95} = 9. This direction corresponds to paleomagnetic poles at the *Lat.* 68°N and *Long.* 161°E, with *K*= 60.1 and A_{95} = 9.9. **(Table 4** and **Figure 18)**. As **Component (B)** was removed before isolating **Component (A)**, the latter is believed to be older and as it heads toward the plot origin up to the end of treatment. **Figure (19)** displays the plots of the corresponding paleomagnetic poles from the two components. When comparing the resultant paleomagnetic pole with further to some selected, reliable African Jurassic and Cretaceous north Paleomagnetic poles (**Table 5** and **Figure 20)**; we found that there is a good agreement between them.

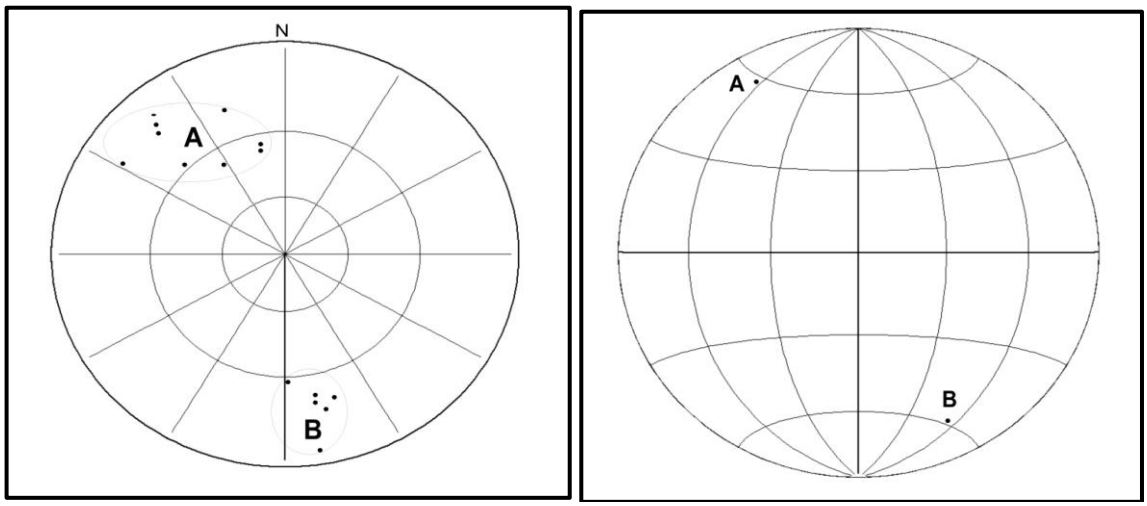

Fig. 16: (Right) Equal-area stereographic projections of site-mean component directions and two components directions from Nigrub El Fogany ring complex.

Fig. 17: (Left) Equal-area projections of the paleomagnetic pole position for the two components (A and B) of Nigrub El Fogany ring complex.

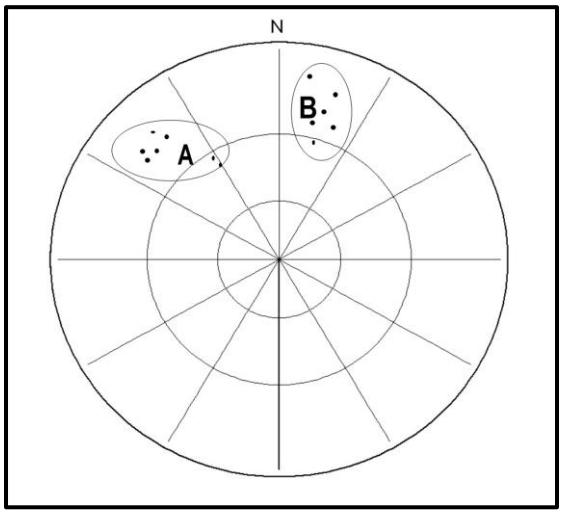

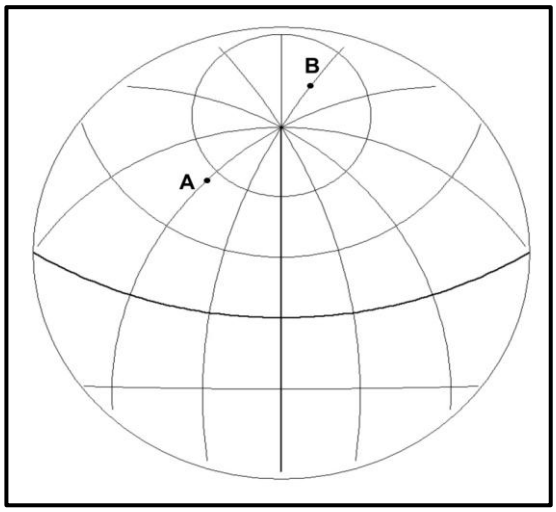

Fig. 18: (Right) Equal-area stereographic projections of site-mean component directions and two component directions from Nigrub El Tahtany ring complex.

Fig. 19: (Left) Equal-area projections of the paleomagnetic pole position for the two components (A and B) of Nigrub El Tahtany ring complex.

Table 5: List of the selected African Jurassic and Cretaceous north Paleomagnetic poles.

Rock unit location reference	Magn. Age (Ma)	Paleopole Long. Lat.	A_{95} or α_{95}
Abu Khruq & El Kahfa, Egypt. Lotfy, 1995	90	266.0 53.0	9.0
Abu Rawash sediments, Egypt. Kafafy et al., 1994	Turonian	230.0 61.0	12.0
Chalk Formation, El Bahariya. Abd El- All, 1998	Maastrichtian	290.0 60.0	13.0
El Bahariya Formation, El Bahariya Oasis, Egypt. Abd El- All, 1998	L-Cenonian	267.0 77.0	9.8
El Geiz Formation, El Bahariya Oasis, Egypt. Abd El- All, 1998	U-Cenonian	220.0 79.0	8.0
El Hefuf Formation, El Bahariya Oasis, Egypt. Abd El- All, 1998	Turonian-Santonian	270.0 73.0	4.7
El Naga Ring Complex, Egypt. Abd El- All, 2004	~140	268.0 69.0	5.0
Mishbeh Ring Complex, Egypt. Mostafa, R, 2010	~142	291.0 58.0	3.7
Nigrub El Fogani Ring Complex, Egypt. This study	*~139*	*296.0 54.0*	*12.7*
Nigrub El Tahtani Ring Complex, Egypt. This study	*~140*	*298.0 49.0*	*9.0*
Wadi Natash volcanics, Egypt. Schult et al., 1981	Kl	258.1 69.3	8.5
Wadi Natash volcanics, Egypt. Ressetar et al., 1981	Kl	251.8 64.6	4.6
Lupata lavas, Mozambique. Gough & Opdyke, 1963	Kl	251.6 69.1	4.0
Mlanje Massivf, Malawi. Briden, 1967	Kl	255.9 67.4	12.0
Kaoka laves, Namibia. Gidskehauge et al., 1975	Kl	262.8 55.8	3.1
Kimberlite, South Africa. Hargraves, 1989	Kl	266.7 55.2	9.7
Djebel Oust, Tunisia. Nairn et al., 1981	Ju	200.3 65.2	6.1
Hodh Dolerite, Mauritania. Sichler et al., 1980	Jl	240.0 71.0	6.1
Hank Dolerite, Mauritania. Westphal et al., 1979	Jl	232.0 69.0	4.1
Volcanics, Liberia. Dalrymple et al., 1975	Jl	242.0 69.0	5.3
Intrusives, Nigeria. Márton & Márton, 1976	Jl	242.0 62.0	13.0
Foam Dykes, Morocco. Hailwood & Mitchel, 1971	Jl	259.0 58.0	4.0
Draa Sills, Morocco. Hailwood & Mitchel, 1971	Jl	230.0 66.0	4.0
Intrusives, Morocco. Bardon et al., 1973	Jl	216.0 71.0	7.0

Mateke Complex, Zimbabwee. Gough & Brock, 1964	Jl	253.2 65.9	7.9
Shawa ijolite, Zimbabwee. Gough & Brock, 1964	Jl	260.6 71.5	14.1
Lesotho Stormberg, South Africa. Van Zijl et al., 1962	Jl	263.6 78.5	14.5
Hoachana Lavas, South West Africa. Gidskehaug et al., 1975	Jl	245.4 68.0	7.0
Marangudzi Complex, Zimbabwee. Brock, 1968	Jl	289.1 77.3	9.0
Karro Dolorite, Mozambique. Mcelhinny & Jones, 1965	Jl	245.2 72.0	12.0
Karro Lavas, Mozambique. Mcelhinny et al., 1968	Jl	258.9 64.4	8.0

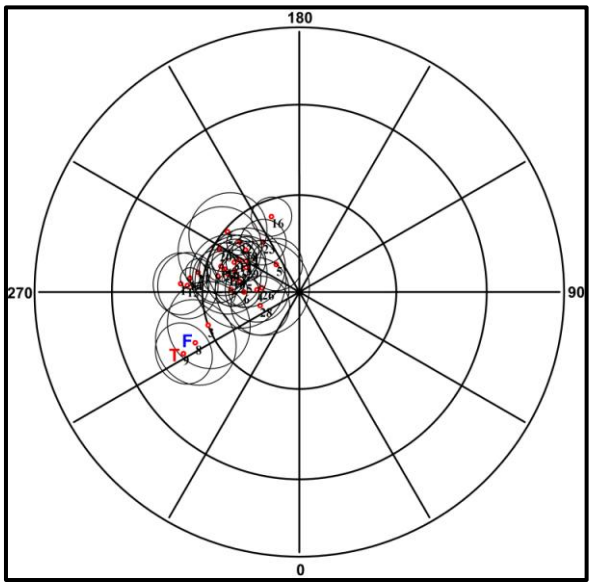

Fig. 20: Jurassic- Cretaceous paleomagnetic-pole positions of Africa.
F: denotes the pole for Nigrub El Fogany Ring Complex
T: denotes the pole for Nigrub El Tahtany Ring Complex

V. DISCUSION

The results obtained from the rock magnetic studies of Nigrub El Fogany ring complex; reveal the coexistence of goethite of very low blocking temperature; magnetite and titanium rich titanomagnetite that changes at high temperature into hematite, titanomagnetite is the main carrier of NRM.

Based on the results of thermal and AF-demagnetization, a low coercive, intermediate (<580°C) unblocking temperature magnetic mineral (titanomagnetite) has been identified as the principle carrier of the high temperature component of pseudo-single domain (PSD) grain size with traces of hematite.

The ChRM component isolated from Nigrub El Fogany ring has an overall mean direction of *D/I* = 323°/25°, with *k* = 17 and α_{95} = 11.9°. This direction corresponds to a paleomagnetic pole at *Lat.* 54°N and *Long.* 296°E, with *K*= 17.4 and A_{95} = 12.7. Due to its high stability, high unblocking temperature and consistent directions, it is considered as of primary origin.

For Nigrub El Tahtany ring complex, the results obtained from the rock magnetic studies reveal the coexistence of goethite of very low blocking temperature, oxidation of titanomagnetite to hematite and magnetite. Based on the results of thermal and AF-demagnetization, titanomagnetite of very low blocking temperature is the carrier of serious part of intensity of pseudo-single domain (PSD) grain size. The primary component has an overall mean ChRM direction *D/I* = 318°/25°, with *k* = 46 and α_{95} = 8.8. This direction corresponds to a paleomagnetic pole at *Lat.* 49°N and *Long.* 298°E, with *K*= 45.6 and A_{95} = 9.

The magnetic susceptibility of Nigrub El Fogany and Nigrub El Tahtany ring complexes are low and variable. This indicates a variation in content and type of the ferromagnetic minerals and, consequently, different types of the AMS. The anisotropy degree *P'* is low, average of 4.0%, and 2.0% for Nigrub El Tahtany ring complexes which indicate a very low deformation. The magnetic foliation is predominant over lineation in most parts from the three rings.

The bulk AMS axial distribution together with the weakly developed magnetic fabrics indicate that the magnetic fabric is most probably of primary origin with respect to the original emplacement process through magma flow with subsequent cooling and further crystallization in a weak compression condition. Such results support the paleomagnetic interpretation and give much confidence in the presumed primary nature of obtained paleomagnetic pole.

ACKNOWLEDGEMENT

We are greatly indebted to the staff member of Paleomagnetic laboratory of Geophysical Institute in Warsaw, Poland and Department of Earth and Planetary Science, University of Tokyo, Japan, for their help and permission for using their laboratories.

REFERENCES

[1]. **Abd El-All, E. (1998):** A paleomagnetic study of the Upper Cretaceous rocks from El- Bahariya Oasis, Western Desert, Egypt**.** Delta J. Sci. 22: 100-126.
[2]. **Abd El-All, E. (2004):** Rock magnetic and paleomagnetic study of Triassic rocks from El-Gezira ring complex, South Eastern Desert, Egypt. Jour. of Petroleum and Mining Engineering (JPME), 6: 49-63.
[3]. **Bardon, C., Bossert, A., Hamzeh, R. and Westiphal, M. (1973):** Etude paleomagnetique de formations du Trias et du Jurassique du Maroc et du Sahara. C. R. Acad. Sci. Paris, 276D: 2357-2360.
[4]. **Briden, J. C. (1967):** A new paleomagnetic results from the Lower Cretaceous of East-Central Africa. Geophys. J. R. Astr. Soc., 12: 375-380.
[5]. **Brock, A. (1968):** Paleomagnetism of the Nuanetsi Igneous Province and its bearing upon the sequence of Karroo igneous activity in Southern Africa. J. Geophys. Res., 73: 1389-1397.
[6]. **Dalrymple, G. B., Gromme, C. S. and White, R. W. (1975):** Potassium-argon age and paleomagnetism of diabase dykes in Liberia: Initiation of central Atlantic rifting. Geol. Soc. Am. Bull., 86: 399-411.
[7]. **Day, R., Fuller, M.D. and Schmidt, V.A. (1977):** Hysteresis properties of titanomagnetites: Grain size and composition dependence. Phys. Earth Planet. Intr., 13: 260-267.
[8]. **El-Ramly, M. F. (1963):** The absolute ages of some basement rocks from Egypt: U. A. R. Ministry of Industry Geological survey and Mineral Research Dept., 15.
[9]. **El-Ramly, M. F., Budanov, V.I., Armanious, L. K. and Dereniuk, N. E. (1969):** The Three Ring Complexes Of The Gabal El Kahfa, Gabal Nigrub El Fogany And Gabal El Naga. Geol. Surv. Egypt, 52, 111pp.
[10]. **El-Ramly, M. F., Budanov, V.I., Hussein, A. A. (1971):** The alkaline rocks of South Eastern Desert. Geol. Surv. Egypt, 53: 111p.
[11]. **El-Ramly, M. F., Armanious, L. K. and Hussein, A. M. (1979):** The two ring complexes of Hadayib and Um Risha, south Eastern Desert. Ann. Geol. Surv. Egypt, 9: 61-69.
[12]. **El Ramly, M. F. and Hussein, A. A. (1984):** The ring complexes of the Eastern Desert of Egypt, Ann. Geol. Surv. Egypt, 1-5.
[13]. **Fisher, R. A. (1953):** Dispersion on a sphere. Proc. Roy. Soc., 217: 295-305.
[14]. **Fleck, R. J., Coleman, R. G., Cornwal, H. R., Greenwood, W. R., Hardley, D. C., Prinz, W. C., Ratte, J. S. and Schmidt, D. L. (1976):** Potassium- Argon geo-chronology of the Arabian shield. Bull. Geol. Soc. Am., 87: 9-21.
[15]. **Foland, K. A. and Faul, H. (1977):** Ages of the White Mountain intrusives: Am. J. Soci., in press.
[16]. **Gidskehauget, A. Creer, K. M. and Mitchell, J. G. (1975):** Paleomagnetism and k-Ar ages of Southwest African basalts and their bearing on the time of rifting of the South Atlantic Ocean. Geophys. J. R. Astr. Soc., 42: 1-20.
[17]. **Gough, D. I. and Opdyke, N. D. (1963):** The paleomagnetism of the Lupata alkaline Volcanics. Geophys. J. R. Astr. Soc., 7: 457-468.
[18]. **Gough, D. I. and Brock, A. (1964):** The paleomagnetism of the Shawa ijoilie. J. Geophys. Res., 69: 2489-2493.
[19]. **Hailwood,E. A. And Mitchell, J. G. (1971):** The paleomagnetic and radio-metric data results from Jurassic intrusions in South Morocco, Geophys. J. R. Astr. Soc., 24: 351-364.
[20]. **Hargraves, R. B. (1989):** Paleomagnetism of Mesozoic Kimberlites in SouthernAfrica and the Cretaceous apparent polar wander curve for Africa J. Res., 94: 1851-1866.
[21]. **Kafafy, A. M., Tarling, D. H., El-Gamili, M. M., Hamama, H. H. and Ibrahim, E. H. (1994):** Contribution to the Cretaceous–Tertiary Paleomagnetism in the Nile Vally, Egypt. Proc. Egypt Acad. Sci., 45: 121-139.
[22]. **Kirschvink, J. L. (1980):** The least squares line and planes and the analysis of paleomagnetic data. Geophys. J. R. Astr.Soc., 62: 699-718.
[23]. **Klerkx, J. and Rundle, C. (1976):** Preliminary K/Ar ages of different igneous rock formations
[24]. from Gebel Uweinat region (SE Libya). Rapp. Ann. (1975), Mus. Roy. Afr. Central, Dep.
[25]. Geol. Min., Tervuren: 105-111.
[26]. **Lotfy, H. I. (1995):** The orientation and paleolatitude of the northeastern part of African Plate during the Upper Cretaceous: A paleomagnetic study on the Upper Cretaceous ring complexes in the Central Eastern Desert of Egypt. Abs. 33rd ann. meeting Egyptian Geol. Society.
[27]. **Marsh, J. S. (1973):** Relationships between transform directions and alkaline igneous rock lineaments in Africa and South America: Earth Planet. Sci. Lett. 18: 317-323.
[28]. **Márton, E. and Márton, P. (1976):** A paleomagnetic study of the Nigerian volcanic provinces. Pure Appl. Geophys., 114: 61-69.
[29]. **McElhinny, M. W. and Jones, D. L. (1965):** Paleomagnetic measurements on some Karroo dolerites from Rhodesia. Natyre, 206: 921-922.
[30]. **McElhinny, M. W., Briden, J. C., Jones, D. L. and Brock, A. (1968):** Geological and geophysical implications of Paleomagnetic results from Africa. Rev. Geophys., 6: 201-238.
[31]. **Mostafa, R. (2010):** Palaeomagnetism of some ring complexes from south eastern desert, Egypt, Ph. D. Thesis, 150-152**.** or 188pp.
[32]. **Nairn, A. E. M., Schmitt, T. J. and Smithwick, M. E. (1981):** A paleomagnetic study of the Upper Mesozoic succession in Northern Tunisia. Geophys. J. R. astr. Soc., 65: 1-18.
[33]. **Neary, C. R., Gass, G. and Cavanach, B.J. (1976):** Granitic association of northeastern Sudan. Bull. Geol. Soc. Am. 87: 1502-1512.
[34]. **Ressetar, R, Nairn, A. E. M. and Monrad, J. R. (1981):** Two phases of Cretaceous-Tertiary magmetism in the Eastern desert of Egypt: paleomagnetic, chemical and K-Ar evidence. Tectonophysics, 73: 169-193.
[35]. **Schult, A., Hussian, A. G. and Soffel, H. C. (1981):** Paleomagnetism of Upper Cretaceous Volcanics and Nubian sandstone of Wadi Natash, SE Egypt and implications for the polar wonder path for Africa in the Mesozoic. J. Geophys., 50: 16-22.
[36]. **Sichler, B., Olivet, J. L., Auzende, J. M., Jonquet, H., Bonnin, J. and Bonifay, A. (1980):** Mobility of Morocco. Can. J. Earth Sci., 17: 1546-1588.
[37]. **Van Zijl, J. S. V., Graham, K. W. T. and Hales, A. L. (1962):** The paleomagnetism of the Stormberg lavas II, The behaviour of the magnetic field during a reversal. Geophys. J. R. Astr.Soc., 7: 169-182.
[38]. **Vail, J. R. (1968):** Outline of the Geology and mineral deposits of the Democratic Republic of the Sudan and adjacent areas. Overseas Geol. And Mineral Resources 49:1-66.

[39]. **Westphal, M., Montigny, R., Thuizat, R., Bardon, C., Bosttert,A., Hamzeh, R. and Rolley, J. P. (1979):** Paleomagnetisme et datation du volcanisme permien, Triasique et crtace du Maroc. Can. J. Earth Sci., 16: 2150-2164.
[40]. **Zijderveld, J. D. A. (1967):** AC demagnetization of rocks: analysis of results. In: Collinson, D. W., Creer, K. M., Runcorn, S. K. (Eds.), Methods in Paleomagnetism. Elsevier, Amesterdam, New York, 254-286.